Integrative and Comparative Biology, volume 51, number 6, pp. 957–968
doi:10.1093/icb/icr034

SYMPOSIUM

Shake Rattle and Roll: The Bony Labyrinth and Aerial Descent in Squamates

Renaud Boistel,[1,*] Anthony Herrel,[1,2,†] Renaud Lebrun,[‡] Gheylen Daghfous,[†] Paul Tafforeau,[§] Jonathan B. Losos[¶] and Bieke Vanhooydonck[||]

*IPHEP-UMR CNRS 6046, UFR SFA, Université de Poitiers, 40 avenue du Recteur Pineau, F-86022, Poitiers, France; [†]UMR 7179C.N.R.S/M.N.H.N., Département d'Ecologie et de Gestion de la Biodiversité, 57 rue Cuvier, Case postale 55, 75231, Paris Cedex 5, France; [‡]Institut des sciences de l'évolution, Université Montpellier 2 – CNRS, CP 64, Place Eugène Bataillon, 34095 Montpellier Cedex 5, France; [§]European Synchrotron Radiation Facility, 6 Rue Jules Horowitz, BP 220, 38043 Grenoble, Cedex 9, France; [¶]Harvard Museum of Comparative Zoology, 26 Oxford St., Cambridge, MA 02138, USA; [||]Deptartment of Biology, University of Antwerp, Universiteitsplein 1, B-2610 Antwerpen, Belgium

From the symposium "The Biomechanics and Behavior of Gliding Flight" presented at the annual meeting of the Society for Integrative and Comparative Biology, January 3–7, 2011, at Salt Lake City, Utah.

[1]These two authors contributed equally to this work.

[2]E-mail: anthony.herrel@mnhn.fr

Synopsis Controlled aerial descent has evolved many times independently in vertebrates. Squamates (lizards and snakes) are unusual in that respect due to the large number of independent origins of the evolution of this behavior. Although some squamates such as flying geckos of the genus *Ptychozoon* and the flying dragons of the genus *Draco* show obvious adaptations including skin flaps or enlarged ribs allowing them to increase their surface area and slow down their descent, many others appear unspecialized. Yet, specializations can be expected at the level of the sensory and neural systems allowing animals to maintain stability during controlled aerial descent. The vestibular system is a likely candidate given that it is an acceleration detector and is well-suited to detect changes in pitch, roll and yaw. Here we use conventional and synchrotron μCT scans to quantify the morphology of the vestibular system in squamates able to perform controlled aerial descent compared to species characterized by a terrestrial or climbing life style. Our results show the presence of a strong phylogenetic signal in the data with the vestibular system in species from the same family being morphologically similar. However, both our shape analysis and an analysis of the dimensions of the vestibular system showed clear differences among animals with different life-styles. Species able to perform a controlled aerial descent differed in the position and shape of the inner ear, especially of the posterior ampulla. Given the limited stability of squamates against roll and the fact that the posterior ampulla is tuned to changes in roll this suggests an adaptive evolution of the vestibular system in squamates using controlled aerial descent. Future studies testing for similar differences in other groups of vertebrates known to use controlled aerial descent are needed to test the generality of this observation.

Introduction

Even though powered flight evolved only twice among extant vertebrates, controlled aerial descent is relatively common and has evolved many times independently in amphibians, reptiles and mammals (Dudley et al. 2007). The evolution of controlled aerial descent in many squamates (lizards and snakes) has gone hand-in-hand with elaborate morphological specializations such as skin flaps and webbed feet as observed in the flying geckos of the genus *Ptychozoon* (Marcellini and Keefer 1976; Russell 1979; Young et al. 2002) or elaborate patagia supported by highly elongated ribs as observed in the South–East Asian flying dragons of the genus *Draco* (McGuire 2003; McGuire and Dudley 2005). However, several other species known to be able to perform controlled aerial descents show little or no obvious morphological specialization (Socha 2002; Vanhooydonck et al. 2009; Socha et al. 2010).

Advanced Access publication June 22, 2011

Despite the lack of obvious morphological specialization, the ability to maintain balance and stability during a controlled aerial descent is likely crucial. As such, the nervous system has been implicated in playing an important role in the evolution of animal flight (Maynard-Smith 1952). Given that many squamates show little or no morphological specialization they are likely unstable in the air and adjustments by movements of limbs, tail, and body may be crucially important for maintaining stability and for maneuvering in mid-air (McCay 2001). Associated with the need for fine tuning of movements is the need for highly developed sensory systems able to detect changes in position of the body. The vestibular system is ideally suited to do so as it is composed of detectors of linear and rotational acceleration, velocity, and displacement (Muller 1994; Muller and Verhagen 1988, 2002a,b,c) which have been hypothesized to help maintain stability during flying (Witmer et al. 2003; Necker 2006). As such, the vestibular system has been proposed as a crucially important sensory system in flying, gliding, and even in arboreal mammals given its role in stabilization of gaze in organisms confronted with fast and complicated optic flow (Spoor et al. 2007).

In other vertebrates, correlations between locomotor behavior and the size and shape of the semi-circular canals have been demonstrated (Spoor 2003; Spoor et al. 2007; Walsh et al. 2009; Boistel et al. 2010). Moreover, the vestibular system and specifically the size of the semi-circular canals was demonstrated to be different in primates using rapid jerky movements versus those using slow, continuous locomotion. Similarly, aquatic and terrestrial mammals are known to differ in the size of the semi-circular canals (Spoor 2003; Spoor et al. 2007). This suggests that differences in the size and shape of the vestibular system can be expected based on differences in the magnitude and type of accelerations experienced by animals in their environment and the complexity of body posture and body control. However, recent studies on the morphology and structure of the labyrinth in strepsirrhine primates demonstrated a strong phylogenetic signal that may overshadow any ecological signal present in the data (Lebrun et al. 2010). Squamate lizards may be an ideal system to test for a functional signal in the size and shape of the vestibular system given the importance of stability during controlled aerial descent, and the repeated independent evolution of controlled aerial descent that took place at least six times during the evolution of the group (Dudley et al. 2007; Vanhooydonck et al. 2009).

Here, we explore the correlation between the size and shape of the vestibular system in squamates differing in their locomotor ecology (terrestrial, climbing, and those known to be able to perform controlled aerial descent) using direct measurements and landmark-based methods. To do so, we make use of conventional and synchrotron microtomographic (μCT) scans of a range of species including all species that have been suggested in the literature to use controlled aerial descent.

Materials and methods

Specimens

One specimen each of *Anolis carolinensis* (A. Herrel, personal collection), *Anolis cybotes* (A. Herrel, personal collection), *Anolis pentaprion* (MCZ R-31582), *Coleonyx variegatus* (A. Herrel, personal collection), *Gekko vittatus* (A. Herrel, personal collection), *Ptychozoon kuhli* (A. Herrel, personal collection), *Draco volans* (MCZ R-26153), *Agama agama* (A. Herrel, personal collection), *Phrynocephalus guttatus* (MNHN1975.1469), *Uromastyx acanthinurus* (A. Herrel, personal collection), *Leiolepis belliana* (A. Herrel, personal collection), *Pareas margaritophorus* (MNHN 1974.1469), *Chrysopelea ornata* (MCZ R-177291), *Pantherophis guttatus* (A. Herrel, personal collection), *Holaspis guentheri* (A. Herrel, personal collection), *Psammodromus algirus* (A. Herrel, personal collection) and *Podarcis muralis* (A. Herrel, personal collection) were scanned and used to quantify the structure of the vestibular system.

Conventional and synchrotron microtomography

We used the ID19 and BM5 beamlines of the European Synchrotron Radiation Facility (Grenoble, France) to scan *A. carolinensis*, *C. ornata*, *D. volans*, *H. guentheri*, *P. margaritophorus*, *P. guttatus*, *P. muralis*, *A. agama*, *A. cybotes*, *P. guttatus*, and *P. kuhli*. The reconstruction was performed using the filtered back-projection algorithm (PYHST software, European Synchrotron Research Facility). In addition we scanned specimens of *L. belliana*, *C. variegatus*, *G. vittatus*, *P. algirus*, *U. acanthinurus* on a Viscom system at the University of Poitiers and a specimen of *A. pentaprion* on an XRA-002 microCT scan (X-Tek) available at the Center for Nanoscale Systems at Harvard University. Voxel sizes varied between 5.06 and 45.88 μm depending on the type of scan and the size of the specimen.

Three-dimensional processing and rendering was obtained after semi-automatic segmentation of the

cranial skeleton and vestibular system using gensurface in AVIZO 6.3 (VSG, Burlington MA, USA). Geometrical and quantitative measurements on the sample were performed with IMAGEJ (available from http://rsb.info.nih.gov/ij).

Morphometric analysis

Using the reconstructed heads of all the species we extracted the 3D coordinates of a number of points in Avizo 6.3 (Figs. 1 and 2; Supplementary Figs. 1 and 2) which were used to calculate the following dimensions and angles using avisoDataParser:

(1) Vestibular systems were measured on the left inner ear (Fig. 1). The vertical and horizontal diameters of each semicircular canal (anterior, horizontal, posterior) were calculated by taking coordinates on surface renderings at the middle of each canal. For each ampulla (anterior, horizontal, posterior), we took the coordinates describing the greatest length, width, and height (Fig. 1). We also took coordinates describing the length, and the antero-posterior and medio-lateral diameter of the common duct. Finally, we quantified the size of the utriculus by taking the coordinates of points describing its greatest length, vertical diameter and horizontal diameter.

(2) Angular dimensions of the vestibular system (Fig. 2) included the angle between the anterior and posterior semi-circular canals; the angle between the anterior canal and the ampulla; the angle between the anterior ampulla and the horizontal canal; the angle between the posterior canal and the ampulla; the angle between the posterior ampulla and the common duct; the angle between the posterior ampulla and the utriculus; and the angle between the common duct and the utriculus.

(3) Overall inner-ear dimensions were calculated as follows (Supplementary Fig. 1): inner-ear length was based on landmark coordinates describing the maximum length between the anterior and posterior semi-circular canals; minimum width between the pair of inner ears at the narrowest point; maximum width between the two inner ears at the widest point; inner ear width at the widest point, and inner ear height between the cochlear apex and apex of the common duct.

(4) External measurements of the skull (Supplementary Fig. 2) were calculated using

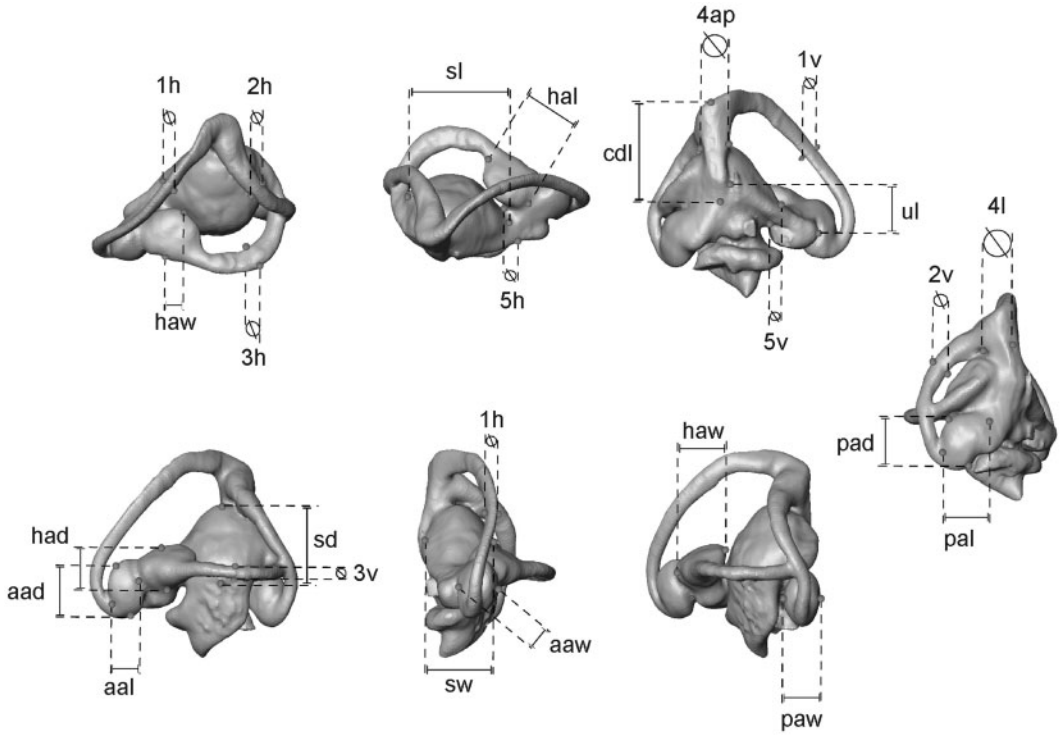

Fig. 1 The linear dimensions and diameters quantified for the vestibular system as exemplified by the left vestibular system in *L. belliana*. Illustrated in clockwise fashion are: a dorso-lateral view, a dorso-medial view, a medial view, a caudal view, a caudal view in the plane of the posterior canal, a frontal view in the plane of the anterior canal, and a lateral view. See 'Materials and methods' section and Table 1 for a list of abbreviations.

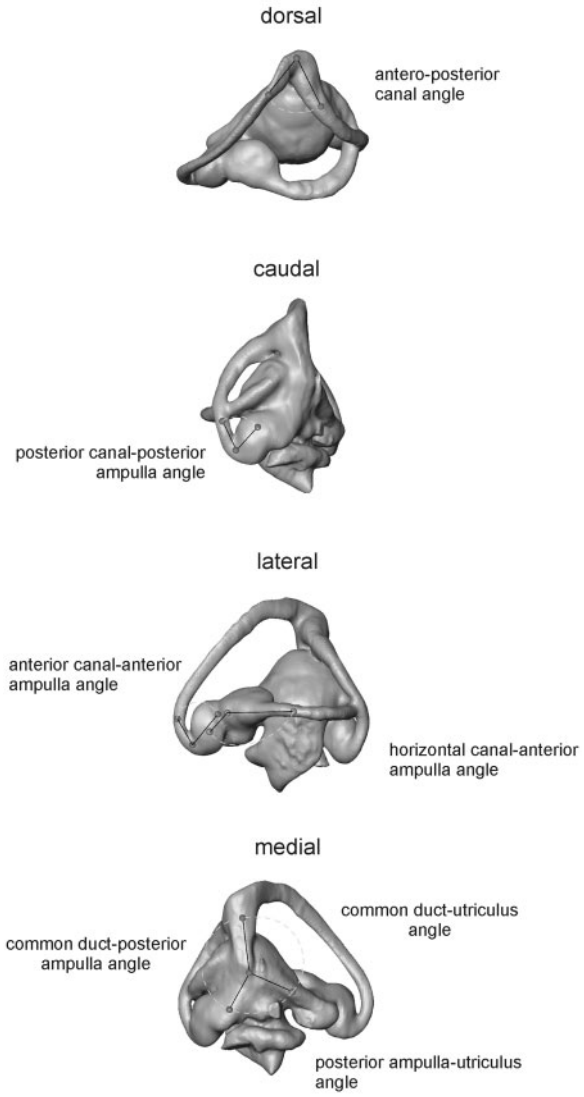

Fig. 2 The angles taken by the vestibular system. On the left is the vestibular system of *L. belliana* in dorsal, caudal, lateral, and medial view.

the coordinates of landmarks: length from the tip of the snout (premaxilla) to the apex of the occipital condyle; width of the skull at its widest point; height of the skull between the posterior aspect of the parietal window and the ventral aspect of the basisphenoid.

The shape of the vestibular system was quantified using 19 anatomical landmarks distributed approximately equally over the entire inner ear as follows: (1) the oval window, (2) the round window, (3) the endolymphatic duct, (4) the apex of the cochlea, (5) the apex of the common duct, (6) the ampulla of the lateral canal, (7) the posteromedial-most point of the lateral canal, (8) the posterolateral-most point of the lateral canal, (9) the anterolateral-most point of the lateral canal, (10) the ampulla of the anterior canal, (11) the superior-most point of the anterior canal, (12) the medial-most point of the anterior canal, (13) the inferior-most point of the anterior canal, (14) the ampulla of the posterior canal, (15) the inferior-most point of the posterior canal, (16) the superior-most point of the posterior canal, (17) the posteromedial-most point of the posterior canal, (18) the posterior sinus, and (19) the intersection between the lateral canal and the sacculus (Fig. 3). As a single threshold value could affect to some extent the reconstruction of the semicircular canals (Spoor and Zonneveld 1995), landmarks were located at the centers of the lumina of the semicircular canals and of the ampullae. Central locations were determined by means of the medial axis transform (Amenta et al. 2001) known as ''skeletonization.'' This procedure reduces a 3D object volume (such as the endocast of the bony labyrinth) to a set of connected lines, whereby each line point represents a local centre of the object. Most landmark locations were defined relative to the three main axes of the labyrinth (Fig. 3). Additional landmark locations were defined at centers of anatomical structures (the ampullae of the semicircular canals, the endolymphatic duct, the cochlear apex, and the oval and round windows), and at the bifurcation of the common duct (Fig. 3).

Using generalized least-squares fitting (Rohlf 1990) and principal components analysis (PCA) of shape (Dryden and Mardia 1998), the form of each specimen's landmark configuration was represented by its centroid size, and by its multi-dimensional shape vector in the linearized Procrustes shape space. Analysis and visualization of patterns of variation in shape were performed with the interactive software package MorphoTools (Specht et al. 2007; Lebrun et al. 2010). To test whether the shape of the vestibular system differs among species characterized by different locomotor ecologies, we used a linear discriminant analysis on the PC scores of the specimens, using locomotor ecology as the categorical variable.

Statistical analysis

All morphometric data were $\log_{10}$ transformed prior to analyses to meet assumptions of normality and homoscedascity required for parametric analyses. As species are not independent data points but related through their evolutionary history, we used phylogenetically informed analyses. Given the large number of measurements taken in the vestibular system of

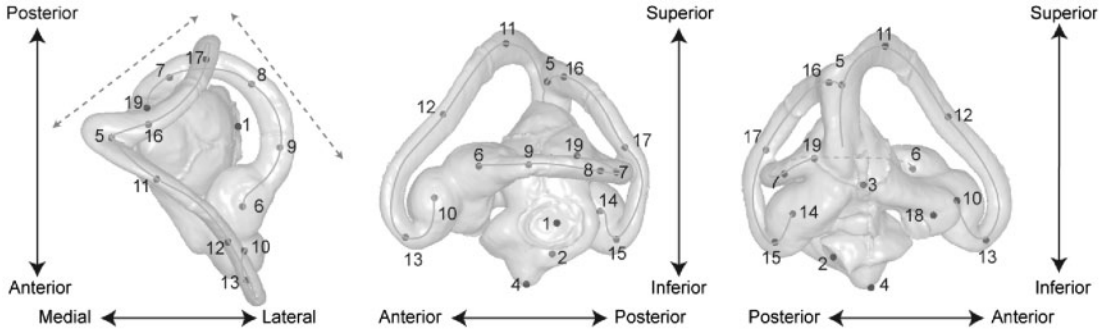

Fig. 3 Landmarks used for geometric morphometric analysis of the inner ear, as exemplified by *A. agama*. Gray arrows: anteromedial-to-posterolateral and anterolateral-to-posteromedial directions used to define landmark locations 7, 8, and 9. The superior-to-inferior direction was used to define landmark locations 11, 13, 15, 16. The gray line represents a simplified version of the medial axis.

each species we first performed a factor analysis with varimax rotation and saved factor scores as new variables to be used in phylogenetic AN(C)OVA's. The phylogenetic framework for these analyses (Fig. 4) was based on Lee (2009) for the interfamilial relationships and on Arnold (1989), Nicholson et al. (2005), Gamble et al. (2008), Collar et al. (2010), and Pyron et al. (2011) for within-families relationships. All branch lengths were set to 1 as branch lengths were not available for all taxa included in our analysis. To check whether branch lengths of unit length were indeed appropriate for our analyses, we used the diagnostics options in the PDTREE program to test for correlations between the absolute values of the standardized contrasts and their standard deviations (Garland et al. 1992). As correlations were not significant, these branch lengths could be used (Garland et al. 1992). Moreover, it has been shown that the actual length of the branches does not usually have substantial effects on the results of phylogenetic analyses (Martins and Garland 1991; Diaz-Uriarte and Garland 1998).

To test whether the structure of the vestibular system of among terrestrial species, climbing species, and those employing controlled aerial descent differed, we ran phylogenetic analyses of (co)variance involving simulation analyses using the PDSIMUL and PDANOVA programs (Garland et al. 1993). In the PDSIMUL program, we used Brownian motion as our model for evolutionary change and ran 1000 unbounded simulations to create an empirical null distribution against which the *F*-value from the original data could be compared. In the PDANOVA program, habitat use was entered as the dependent variable; factor scores and length, width and depth of the skull were used as independent variables. Skull length was used as a covariate when appropriate (i.e. in analyses of skull width and depth). We considered differences among categories to be significant if the original *F*-value derived from a non-phylogenetic analysis was higher than the F95 value derived from the empirical distribution. We ran two analyses on the data, the first one contrasting three groups (terrestrial, climbing, and gliding species) and the second one contrasting "gliding" with non-gliding squamates. Using data from the literature (Oliver 1951; Marcellini and Keefer 1976; Russell 1979; Losos et al. 1989; Manthey and Grossmann 1997; Socha 2002; Young et al. 2002; McGuire 2003; McGuire and Dudley 2005; Vanhooydonck et al. 2009) and from personal observations (*A. pentaprion*), species were classified as to their ability to perform controlled aerial descent. All traditional (i.e. non-phylogenetic) analyses were performed with SPSS v.15.

Results

A factor analysis performed on the measurements taken on the vestibular system of the different species extracted six factors with eigenvalues greater than one, jointly explaining ~91% of the variation in the data (Table 1). The first factor was strongly and positively correlated with the dimensions of the ampullae and with the diameter of the canals. The second factor was strongly and positively determined by the overall size of the skull and vestibular system. The third factor was strongly and positively determined by the angle between the posterior ampulla and the common duct and negatively by the angle between the posterior ampulla and the utriculus, suggesting a more vertical connection between the posterior ampulla/canal and the common duct. The fourth factor was strongly negatively determined by the angle between the anterior canal and the

Table 1 Results from a factor analysis performed on the morphometric data

	Factor 1	Factor 2	Factor 3	Factor 4	Factor 5	Factor 6
Eigenvalues	**15.02**	**11.6**	**2.62**	**2.61**	**2**	**1.48**
Percentage of variation explained	**38.52**	**29.76**	**6.71**	**6.68**	**5.13**	**3.8**
Vertical diamerer of the anterior canal (1v)	**0.95**	0.13	−0.09	0.00	0.06	−0.10
Horizontal diameter of the anterior canal (1 h)	**0.87**	−0.01	0.10	0.21	−0.02	−0.18
Vertical diameter of the posterior canal (2v)	**0.92**	0.05	−0.12	0.00	−0.11	−0.07
Horizontal diameter of the posterior canal (2 h)	**0.88**	−0.03	−0.03	0.05	−0.05	−0.35
Vertical diameter of the horizontal canal (3v)	**0.96**	−0.07	0.10	0.08	−0.07	−0.06
Horizontal diameter of the horizontal canal (3 h)	**0.86**	0.03	−0.40	−0.06	−0.16	0.01
Common duct length (cdl)	0.56	**0.78**	−0.09	0.20	−0.04	0.10
Common duct antero-posterior diameter (4ap)	**0.82**	0.38	0.20	0.08	0.19	0.13
Common duct lateral diameter(4 l)	**0.84**	0.32	0.01	0.09	−0.02	0.11
Utriculus length (ul)	0.47	0.63	0.39	0.27	0.29	0.14
Utriculus vertical diameter (5v)	**0.86**	0.24	0.19	0.01	−0.32	0.19
Utriculus horizontal diameter (5 h)	0.67	0.56	−0.07	0.21	0.07	0.34
Anterior ampulla depth (aad)	**0.80**	0.49	−0.21	0.00	0.13	−0.11
Anterior ampulla length (aal)	**0.77**	0.28	0.19	0.10	0.40	0.16
Anterior ampulla width (aaw)	**0.81**	0.49	0.11	0.20	−0.10	0.02
Horizontal ampulla depth (had)	**0.80**	0.43	0.14	0.30	−0.03	−0.08
Horizontal ampulla length (hal)	**0.82**	0.49	0.08	0.06	0.07	0.09
Horizontal ampulla width (haw)	**0.85**	0.48	0.04	0.09	0.04	0.09
Posterior ampulla depth (pad)	**0.76**	0.58	−0.20	−0.06	0.09	−0.02
Posterior ampulla length (pal)	0.61	0.58	0.08	0.01	0.06	0.24
Posterior ampulla width (paw)	**0.81**	0.50	−0.06	0.02	0.11	0.00
Sacculus depth (sd)	0.32	**0.77**	−0.12	0.33	0.09	0.15
Sacculus length (sl)	0.21	0.68	0.15	0.43	0.44	0.20
Sacculus width (sw)	0.43	0.63	−0.30	0.24	−0.13	0.36
Angle between the anterior and posterior canal	−0.31	0.27	−0.12	0.04	**0.83**	0.06
Angle between the anterior canal and anterior ampulla	−0.16	−0.33	−0.06	**−0.84**	−0.16	−0.03
Angle between the anterior ampulla and horizontal ampulla	0.04	0.13	0.22	**0.82**	−0.03	0.04
Angle between the posterior canal and posterior ampulla	−0.57	−0.01	0.12	0.09	0.20	**0.72**
Angle between the posterior ampulla and common duct	−0.24	0.36	**0.82**	0.17	−0.15	0.00
Angle between the common duct_utriculus	0.35	−0.68	0.14	0.13	0.37	0.26
Angle between the posterior ampulla and utriculus	−0.12	0.02	**−0.96**	−0.15	−0.05	−0.07
Minimum distance ear	0.10	**0.88**	−0.03	−0.37	0.09	−0.01
Maximum distance ear	0.35	**0.88**	0.21	0.06	0.08	−0.14
Ear depth	0.38	**0.82**	0.11	0.22	0.18	−0.07
Ear width	0.17	**0.93**	0.08	0.20	−0.04	−0.01
Ear length	0.25	**0.77**	0.28	0.20	0.39	−0.01
Skull length	0.03	**0.82**	0.14	0.15	0.41	0.22
Skull depth	0.31	**0.84**	0.05	0.08	0.00	−0.13
Skull width	0.08	**0.72**	0.15	0.35	−0.01	0.32

Notes. Abbreviations between brackets refer to abbreviations used in Fig. 1. Bolded values represent loadings greater than 0.7.

anterior ampulla and positively by the angle between the anterior ampulla and the horizontal ampulla. The fifth factor was strongly influenced by the angle between the anterior and posterior semi-circular canals and the sixth factor by the angle between the posterior canal and the posterior ampulla.

A phylogenetic analysis of variance using the factor scores as input and testing for differences in

Table 2 Phylogenetic AN(C)OVA's with species grouped in three (glider, climbing, terrestrial) or two (glider, non-glider) ecological categories

	Three groups			Two groups		
	F	F_{phyl}	P_{phyl}	F	F_{phyl}	P_{phyl}
Factor 1	0.85	1.64	0.18	0.18	1.81	0.49
Factor 2	0.41	1.83	0.44	0.34	2.03	0.38
Factor 3	4.89	1.56	0.002**	4.14	1.84	0.008*
Factor 4	0.11	1.87	0.80	2.44	1.96	0.036*
Factor 5	1.65	1.72	0.057	0.67	1.88	0.21
Factor 6	1.93	1.54	0.027*	0.06	1.87	0.68
Skull length	1.24	1.54	0.086	0.62	1.92	0.23
Skull depth	0.43	1.74	0.40	0.46	1.92	0.29
Skull width	0.03	1.88	0.93	1.53	1.92	0.075
Skull depth (ancova)	0.02	1.88	0.95	0.04	2.14	0.77
Skull width (ancova)	5.17	2.03	0.002**	0.89	2.36	0.18

Note. F = critical F-value based on traditional analyses; F_{phyl} = critical F-value based on a simulation taking into account phylogenetic relatedness among species; P_{phyl} = significance of the AN(C)OVA after taking into account the phylogenetic relatedness among species.
*Significant after taking into account phylogenetic relationships.
**Significant after taking into account phylogenetic relationships and after Bonferroni correction.

Table 3 Factor scores for each ecological group

	Factor 1	Factor 2	Factor 3	Factor 4	Factor 5	Factor 6
Terrestrial	0.15 ± 1.24	0.56 ± 1.11	0.33 ± 0.77	0.38 ± 0.64	−0.28 ± 1.44	−0.07 ± 1.14
Gliders	−0.14 ± 1.17	−0.20 ± 0.71	−0.61 ± 0.61	−0.49 ± 1.36	0.27 ± 0.85	0.09 ± 0.80
Climbers	0.00 ± 0.56	−0.44 ± 1.03	0.34 ± 1.39	0.13 ± 0.76	0.01 ± 0.53	−0.01 ± 1.24

Note. Table entries are means ± standard deviations.

the vestibular structure among terrestrial, climbing and "gliding" squamates found significant differences in factors three and six (Table 2). Gliders score lower and terrestrial and climbing species higher on the third factor (Table 3 and Fig. 3), suggesting that "gliders" differ from the other groups by having a more horizontally positioned connection between the posterior ampulla and the common duct. The difference in factor six indicates again a difference between gliders and the two other groups with gliders having a greater angle between the posterior canal and the posterior ampulla. Finally, climbing species had relatively narrow heads for a given head length compared to terrestrial species; gliders were intermediate. An analysis contrasting gliders to non-gliders retained the difference in factor three with gliders scoring lower on this axis and revealed an additional difference in factor 4 with gliders having lower scores than the non-gliders (Table 2). This indicates that gliders are characterized by a smaller angle between the horizontal and anterior ampullae and a greater angle between the anterior canal and the anterior ampulla.

Our landmark-based analysis of shape-demonstrated distinct differences between phylogenetic groups, regardless of locomotor behavior (Fig. 6). Phylogenetic groups are well separated on the first two principal component axes. A linear discriminant analysis performed on PC scores separated species with different life-styles, with squamates capable of controlled aerial descent scoring particularly low on the second discriminant axis (Fig. 7). Arboreal species are intermediate in vestibular shape compared to terrestrial species and those capable of controlled aerial descent (Fig. 6). Species capable of controlled aerial descent have relatively shorter common ducts, rounder anterior semi-circular canals, and all parts of the posterior semi-circular canal tending to converge on the same plane, whereas other species present relatively longer common ducts, elongated anterior semi-circular canals and somewhat twisted posterior semi-circular canals.

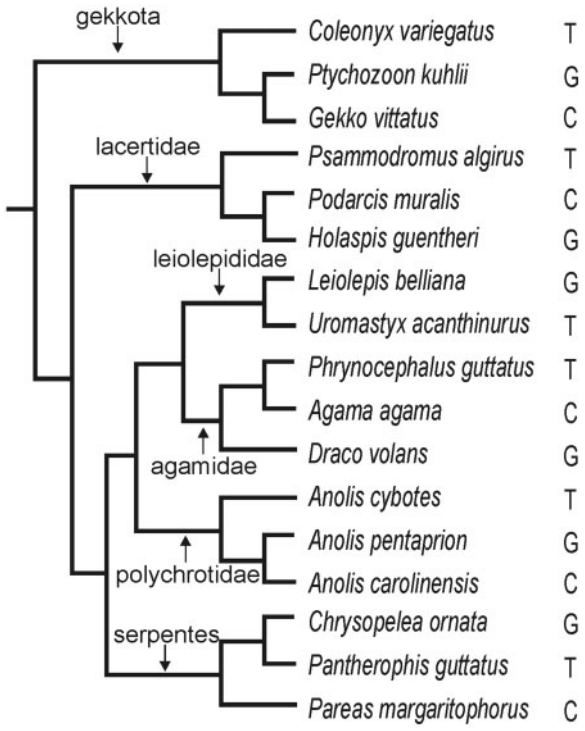

Fig. 4 Composite phylogeny illustrating the phylogenetic relationships between the species used in this study. The ecological classification of each species is indicated one the right. T, terrestrial; C, climbing; G, gliding.

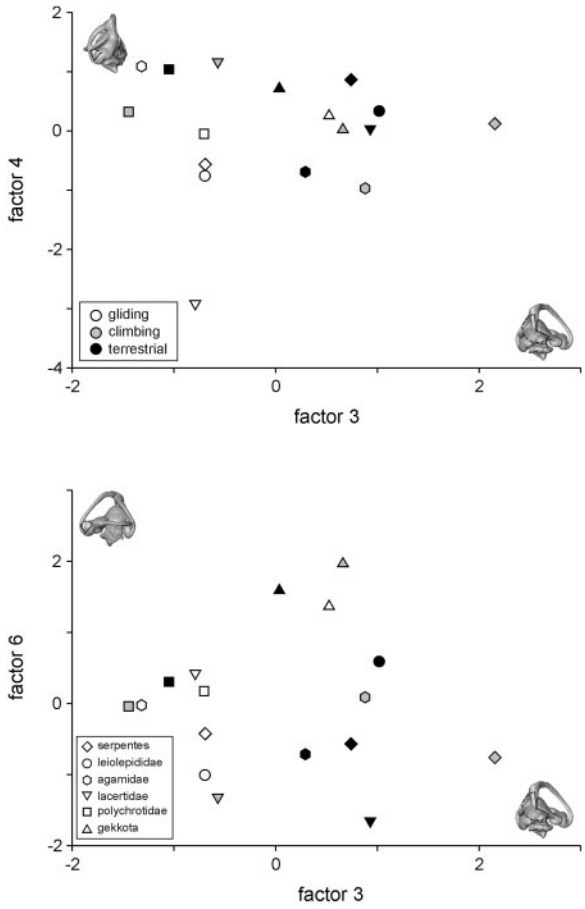

Fig. 5 A factor analysis performed on the $\log_{10}$-transformed measurements illustrating significant differences among three groups of squamates: those capable of performing controlled aerial descent; climbing species; terrestrial species. Only those axes for which differences between ecological groups were significant are illustrated. Open symbols represent gliders, gray symbols climbing species, and black symbols terrestrial species. Symbols represent phylogenetic affinity. Upward triangle, geckos; downward triangle, lacertids; circles, leiolepidids; diamonds, snakes; hexagons, agamids; and squares, *Anolis*. The icons illustrate those angles most contributing to the variation on each axis.

Discussion

Both the factor analysis performed on the raw measurements and the one performed on our landmarks describing variation in shape separate species belonging to the same family in multivariate space. Snakes are especially divergent in having much shallower, less rounded semi-circular canals (Supplementary Fig. 4) compared to the other squamates. Given that the size, that is the radius (Ten Kate et al. 1970) of the semi-circular canals is thought to be related to life-style with more active species having more rounded and larger semi-circular canals, this suggests that snakes, on average, experience lower rotational accelerations. The other interesting group that stands out from the others is lizards of the genus *Anolis*. Indeed, all three species of *Anolis* have very similar morphologies of the inner ear (Figs. 5 and 6) despite marked differences in habitat use and life-style. The agamids also display a rather similar inner-ear shape that is similar to that observed in leiolepidids and *Anolis* (Fig. 6), again demonstrating the strong effect of shared ancestry in driving the morphology of the inner ear in squamates. Interestingly, the effect of shared ancestry appears less strong when quantifying the dimensions of the physiologically relevant structures compared to the landmark-based analysis of shape (compare the panel in Fig. 5 to that in Fig. 7). The presence of a strong phylogenetic signal in the shape of the inner ear and bony labyrinth was previously described for strepsirrhine primates for which it was suggested that inner ear characters may even be used for taxonomic purposes (Lebrun et al. 2010). Interestingly, however, both our factor analysis and our linear discriminant analysis detected significant differences between species with different life-styles and locomotor ecologies.

Indeed, both the overall shape of the bony labyrinth, as well as the angles by which the posterior

ampulla attaches to the common duct, appear to be different among squamates with different modes of locomotion (terrestrial, climbing, controlled aerial descent), even when taking into account the phylogenetic relatedness between species. In contrast to studies on mammals in which the size of the semi-circular canals was demonstrated to be different among species with different life-styles and ecologies (Spoor et al. 2007), the size of the canals did not differ among squamates with different life-styles. Interestingly, most of the differences detected were associated with the angles of the connection between the posterior ampulla and the other structures with which it connects (posterior canal and common duct) (Fig. 5) and to some degree with the angle of the anterior ampulla. The ampulla is a bulbous expansion of the canal which contains a transverse ridge of sensory epithelium called the crista (Selva et al. 2009). The surface of the crista contains the sensory hair cells that detect changes in the movement of the endolymph. The posterior canal is thought to predominantly detect accelerations, velocities, and displacements in the roll and pitch directions (Muller 1994; Muller and Verhagen 2002c). Although unclear how these changes in the angle between the ampullae and the ducts may affect the physiology of the system, any change in the position of the ampulla relative to the canal will likely affect the flow of endolymph and may thus increase the sensitivity of the system. Although studies on frogs suggest that these animals are mostly unstable around the yaw axis, the shape of the body of the squamates, in addition to personal observations of these animals during controlled aerial descents (Vanhooydonck et al. 2009), suggest that they are least stable in the roll direction. If this is indeed the case then an increased sensitivity to roll may

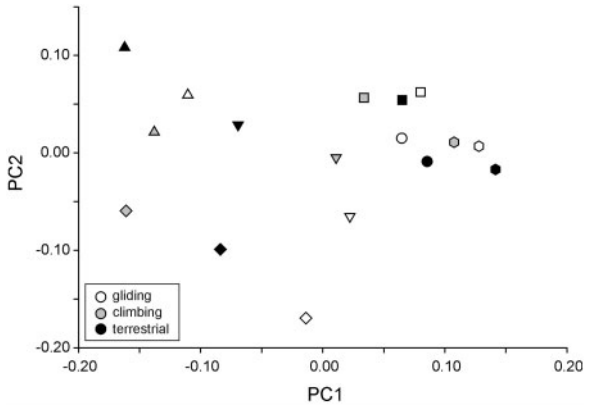

Fig. 6 A principal component analysis performed on the procrustes residuals. Note how species cluster according to their phylogenetic affinity. Gliders (black), climbing species (gray), and terrestrial species (black) are well-separated along the second discriminant axis. Upward triangle, geckos; downward triangle, lacertids; circles, leiolepidids; diamonds, snakes; hexagons, agamids; and squares, *Anolis*.

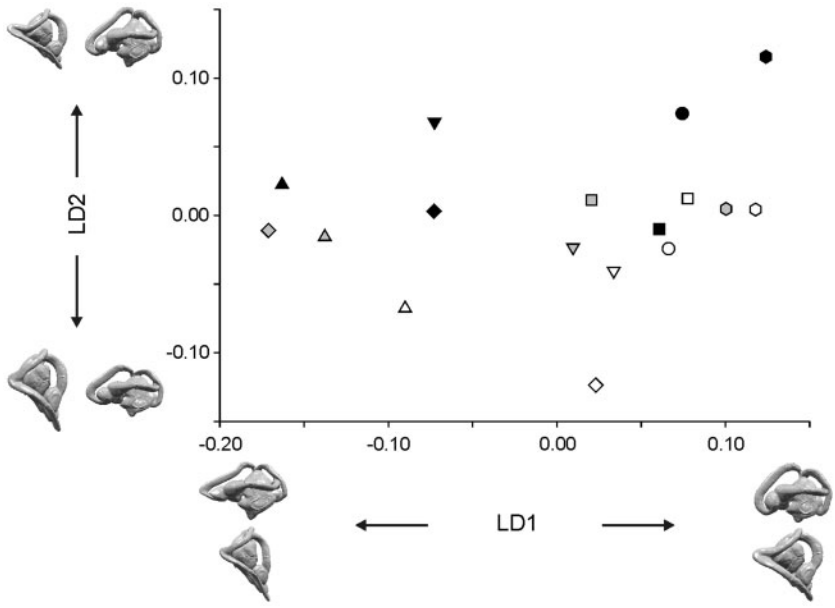

Fig. 7 Results of a linear discriminate analysis performed on the principal component scores. Gliders (black), climbing species (gray), and terrestrial species (black) are well-separated along the second discriminant axis. Icons represent hypothetical vestibular systems in dorsal and lateral view, illustrating the changes in shape along the two discriminant axes. Upward triangle, geckos; downward triangle, lacertids; circles, leiolepidids; diamonds, snakes; hexagons, agamids; and squares, *Anolis*.

be important to correct for deviations from a stable-descent posture that would assure a correct landing. Observations for at least three species of squamates (*H. guentheri*, *P. kuhli*, and *A. pentaprion*) suggest that they often use their tails to try to stabilize themselves against roll during controlled aerial descents (Vanhooydonck et al. 2009; A. Herrel, personal observation), similar to the use of the limbs and tails in gliding mammals such as sugar gliders (Bishop 2007).

Interestingly, the *Anolis* included in our study did not conform to the general pattern observed among squamates. Not only did all *Anolis* species show a morphology similar to that of other squamates capable of controlled aerial descent, but within the *Anolis* species examined the arboreal species was most similar and the "glider" least similar to other "gliding" squamates. Although *A. carolinensis* has been suggested of being able to perform controlled aerial descent (Oliver 1951), which might explain the morphology of its inner ear, *A. cybotes* is unlikely to be able to do so given its large head, stocky body and terrestrial habits. Geckos were also different, with the strictly terrestrial species (*C. variegatus*) being most similar to other squamates capable of controlled aerial descent. Again, however, on average all geckos have an inner ear similar to that observed for "gliders." Given the strong phylogenetic signal in the data, these strange patterns could be the results of the retention of the morphology of an arboreal ancestor. Although this is plausible for *Anolis* (Losos 2009), this is rather unlikely for geckos given the terrestrial habits of the basal-most radiation.

In summary, despite the importance of behavioral adjustments in the evolution of controlled aerial descent, our data suggest that sensory systems may also be tuned to changes in behavior. The structural modifications of the inner ear in species capable of performing controlled aerial descent are likely related to the maintenance of stability. Interestingly, our data show that arboreal taxa have an intermediate inner-ear morphology, suggesting that arboreality may be an important precursor for controlled aerial descent as suggested previously (Dudley et al. 2007). Although our data show differences in the vestibular system in squamates capable of controlled aerial descent, the generality of our findings for other vertebrates remains to be tested. Finally, more detailed studies examining the fine detail and structure of the ampullae are needed. For example, despite its suggested role during aerial behaviors (Harada et al. 2002), the presence of an eminentia cruciata in the ampullae of squamates capable of controlled aerial descent remains to be demonstrated.

Acknowledgments

We would like to thank Filippo Rusconi for letting us use the software (avisoDataParser) he developed to calculate morphological measurements based on 3D coordinate data and Ivan Ineich from the Muséum National d'Histoire Naturelle and Jose Rosado from the Museum for Comparative Zoology for the loan of specimens used in this study. The scan of *A. pentaprion* was performed at the Center for Nanoscale Systems at Harvard University, a member of the National Nanotechnology Infrastructure Network (NSF Award # ECS0335765).

Funding

European Synchrotron Radiation Facility (MD482 to R.B.); the David Rockefeller Center for Latin American Studies, Harvard University; Fund for Scientific Research, Flanders, Belgium (FWO-Vl; postdoctoral fellowship to B.V.).

Supplementary Data

Supplementary data are available at *ICB* online.

References

Amenta N, Choi S, Kolluri R. 2001. The power crust. Proceedings of the sixth ACM symposium on solid modeling and applications. Ann Arbor, Michigan.

Arnold EN. 1989. Towards a phylogeny and biogeography of the Lacertidae: relationships within an old-world family of lizards derived from morphology. Bull Brit Mus Nat Hist 44:291–339.

Bishop KL. 2007. Aerodynamic force generation, performance and control of body orientation during gliding in sugar gliders (*Petaurus breviceps*). J Exp Biol 210:2593–606.

Boistel R, Herrel A, Daghfous G, Libourel P-A, Boller E, Tafforeau P, Bels VL. 2010. Assisted walking in Malagasy dwarf chameleons. Biol Lett 6:740–3.

Collar DC, Schulte JA II, O'Meara BC, Losos JB. 2010. Habitat use affects morphological diversification in dragon lizards. J Evol Biol 23:1033–49.

Diaz-Uriarte R, Garland T Jr. 1998. Effects of branch lengths errors on the performance of phylogenetically independent contrasts. Syst Biol 47:654–72.

Dryden IL, Mardia KV. 1998. Statistical shape analysis. Chichester: John Wiley & Sons.

Dudley R, Byrnes G, Yanoviak SP, Borrell B, Brown RM, McGuire JA. 2007. Gliding and the functional origins of

flight: biomechanical novelty or necessity? Annu Rev Ecol Evol Syst 38:179–201.

Gamble T, Bauer AM, Greenbaum E, Jackman TR. 2008. Evidence for Gondwanan vicariance in an ancient clade of gecko lizards. J Biogeogr 35:88–104.

Garland T Jr, Harvey PH, Ives AR. 1992. Procedures for the analysis of comparative data using phylogenetically independent contrasts. Syst Biol 41:18–32.

Garland T Jr, Dickerman AW, Janis CM, Jones JA. 1993. Phylogenetic analysis of covariance by computer simulation. Syst Biol 42:265–92.

Harada Y, Kasuga S, Tamura S. 2002. Comparison of the morphology of the inner ear between newts and frogs in relation to their locomotor capability. Zool Sci 19:583–92.

Lebrun R, de Leon MP, Tafforeau P, Zollikofer C. 2010. Deep evolutionary roots of strepsirrhine primate labyrinthine morphology. J Anat 216:368–80.

Lee MSY. 2009. Hidden support from unpromising data sets strongly unites snakes with anguimorph lizards. J Evol Biol 22:1308–16.

Losos JB. 2009. Lizards in an evolutionary tree: ecology and adaptive radiation of anoles. Berkeley: University of California Press.

Losos JB, Papenfuss T, Macey JR. 1989. Correlates of running, jumping, and parachuting performance in the butterfly lizard, *Leiolepis belliani*. J Zool 217:559–68.

Manthey U, Grossman W. 1997. Amphibien & reptilian Sudostasiens. Munster: Natur und Tier Verlag.

Marcellini DL, Keefer TE. 1976. Analysis of the gliding behavior of *Ptychozoon lionatum* (Reptilia: Gekkonidae). Herpetologica 32:362–6.

Martins EP, Garland T Jr. 1991. Phylogenetic analyses of the correlated evolution of continuous characters: a simulation study. Evolution 45:534–57.

Maynard-Smith J. 1952. The importance of the nervous system in the evolution of animal flight. Evolution 6:127–9.

McCay MG. 2001. Aerodynamic stability and maneuverability of the gliding frog *Polypedates dennysi*. J Exp Biol 204:2817–26.

McGuire JA. 2003. Allometric prediction of locomotor performance: an example from Southeast Asian flying lizards. Am Nat 161:347–69.

McGuire JA, Dudley R. 2005. The cost of living large: comparative gliding performance in flying lizards (Agamidae: *Draco*). Am Nat 166:93–106.

Muller M. 1994. Semicircular duct dimensions and sensitivity of the vertebrate vestibular system. J Theor Biol 167:239–56.

Muller M, Verhagen JHG. 1988. A new quantitative model of total endolymph flow in the system of semicircular ducts. J Theor Biol 134:473–501.

Muller M, Verhagen JHG. 2002a. Optimization of the mechanical performance of a two-duct semicircular duct system – part 1: dynamics and duct dimensions. J Theor Biol 216:409–24.

Muller M, Verhagen JHG. 2002b. Optimization of the mechanical performance of a two-duct semicircular duct system – part 2: excitation of endolymph movements. J Theor Biol 216:425–42.

Muller M, Verhagen JHG. 2002c. Optimization of the mechanical performance of a two-duct semicircular duct system – part 3: the positioning of the ducts in the head. J Theor Biol 216:443–59.

Necker R. 2006. Specialisations in the lumbosacral vertebral canal and spinal cord of birds: evidence of a function as a sense organ which is involved in the control of walking. J Comp Physiol A 192:439–48.

Nicholson KE, Glor RE, Kolbe JJ, Larson A, Hedges SB, Losos JB. 2005. Mainland colonization by island lizards. J Biogeogr 32:929–38.

Oliver JA. 1951. "Gliding" in amphibians and reptiles, with a remark on an arboreal adaptation in the lizard, *Anolis carolinensis carolinensis* Voigt. Am Nat 85:171–6.

Pyron RA, Burbrink FT, Colli GR, Nieto Montes de Oca A, Vitt LJ, Kuczynski CA, Wiens JJ. 2011. The phylogeny of advanced snakes (Colubroidea), with discovery of a new subfamily and comparison of support methods for likelihood trees. Mol Phyl Evol 58:329–42.

Rohlf FJ. 1990. Rotational fit (Procrustes) Method. In: Rohlf FJ, Bookstein FL, editors. Proceedings of the michigan morphometrics Workshop. Museum of Zoology. The University of Michigan. p. 227–36.

Russell AP. 1979. The origin of parachuting locomotion in gekkonid lizards (Reptilia: Gekkonidae). Zool J Linn Soc 65:233–49.

Selva P, Oman CM, Stone HA. 2009. Mechanical properties and motion of the cupula of the human semicircular canal. J Vest Res 19:95–110.

Socha JJ. 2002. Gliding flight in the paradise tree snake. Nature 418:603–4.

Socha JJ, Miklasz K, Jafari F, Vlachos P. 2010. Non-equilibrium trajectory dynamics and the kinematics of gliding in a flying snake. Bioinsp Biomim 5:1–12.

Specht M, Lebrun R, Zollikofer C. 2007. Visualizing shape transformation between chimpanzee and human braincases. Visual Comput 23:743–51.

Spoor F. 2003. The semicircular canal system and locomotor behavior, with special reference to hominin evolution. Cour Forsch-Inst Senckenberg 243:93–104.

Spoor F, Garland T Jr, Krovitz G, Ryan TM, Silcox MT, Walker A. 2007. The primate semicircular canal system and locomotion. Proc Natl Acad Sci USA 104:10808–12.

Spoor F, Zonneveld F. 1995. Morphometry of the primate bony labyrinth: a new method based on high-resolution computed tomography. J Anat 186:271–86.

Ten Kate JH, van Barneveld HH, Kuiper JW. 1970. The dimensions and sensitivities of semicircular canals. J Exp Biol 53:501–14.

Vanhooydonck B, Meulepas G, Herrel A, Boistel R, Tafforeau P, Fernandez V, Aerts P. 2009. Ecomorphological analysis of aerial performance in a

non-specialized lacertid lizard, *Holaspis guentheri*. J Exp Biol 212:2475–92.

Walsh SA, Barrett PM, Milner AC, Manley G, Witmer LM. 2009. Inner ear anatomy is a proxy for deducing auditory capability and behaviour in reptiles and birds. Proc R Soc B 276:1355–60.

Witmer LM, Chatterjee S, Franzosa J, Rowe T. 2003. Neuroanatomy of flying reptiles and implications for flight, posture and behavior. Nature 425:950–3.

Young BA, Lee CE, Daley KM. 2002. On a flap and a foot: aerial locomotion in the 'flying' gecko, *Ptychozoon kuhli*. J Herpetol 36:412–8.